Downloaded from rsta.royalsocietypublishing.org on October 30, 2010

details). The model correctly reproduced the voltage-dependent slow increase in experimental current relaxation (figure 3*c*(ii)). The time constant of relaxation in the model was also calculated and compared with the experimental data (figure 3*c*(iii)). The time constants of relaxation in simulated data did not show clear voltage dependence and coincided with the experimental data well except at −60 and −80 mV in 0.3 μM ACh where the amplitudes of the relaxation were too small to be accurately assessed.

Figure 3*d* shows the voltage dependence of the K_{ACh} channel relative NP_o in the presence of 0.1 and 0.3 μM $[ACh]_0$. The symbols correspond to the experimental results and the lines are the results calculated from the integrated model. As $[ACh]_0$ was decreased, the K_{ACh} channel relative NP_o decreased especially at depolarized potentials because of the modulated action of RGS proteins represented by the voltage-dependent k_6. The integrated model developed in this study can therefore quantitatively account for the voltage- and ACh-dependence of the K_{ACh} current relaxation behaviour.

Figure 4*a* shows experimental data examining the effects of prepulse (+40 mV) duration on the relaxation behaviour of the K_{ACh} current at −100 mV. As $[ACh]_0$ was increased, the instantaneous component increased and the time-dependent relaxation component became smaller. This may indicate that the effects of RGS proteins are attenuated as $[ACh]_0$ is increased. At each $[ACh]_0$, as the duration of prepulse was prolonged, the instantaneous component decreased and the relaxation component increased. This implies that the effect of the RGS protein action develops in a time-dependent manner during the prepulse, because the instantaneous component reflects the K_{ACh} channel NP_o at the end of the prepulse. In GTPγS-loaded atrial cells, the prepulse duration did not affect the K_{ACh} current. This is consistent with the idea that the effect of prepulse duration on K_{ACh} current is mediated by the voltage- and time-dependent action of RGS proteins.

In figure 4*b*(i)(ii), the temporal characteristics were extracted from the experimental data by normalizing relative to the data obtained with GTPγS. The normalized currents clearly demonstrated the prepulse duration-dependent development of relaxation (figure 4*b*, dotted lines). The model correctly reproduces the experimental results (figure 4*b*(iii)(iv)). Both the model and experimental results also showed that the alterations of the instantaneous and relaxation components depend on $[ACh]_0$. Therefore, the model successfully replicates the characteristics of K_{ACh} channel current relaxation.

(iii) *The temporal and steady-state behaviour of ACh-induction of K_{ACh} current*

Figure 5*a* shows the temporal behaviour of the ACh-induced K_{ACh} channel current simulated with the improved integrated model. When ACh was applied, the K_{ACh} current was induced with a time constant of 2–8 s. Upon removal of ACh from the external solution, the K_{ACh} current was deactivated with a time constant of 6–12 s. These values are similar to those in physiological activation and deactivation and much smaller than those calculated with the previous models which do not take the voltage-dependent RGS action into account. In the simulated K_{ACh} currents, differences in the activation time course at different membrane potentials were not obvious, while those in the deactivation time

Downloaded from rsta.royalsocietypublishing.org on October 30, 2010

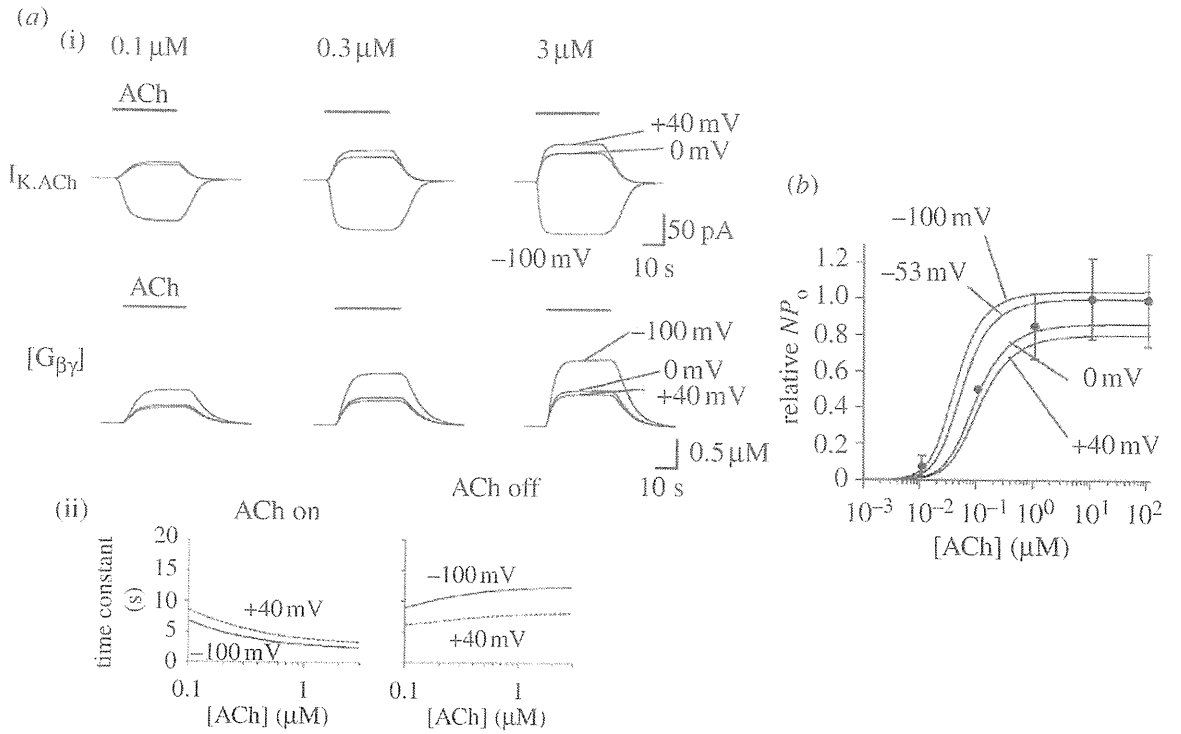

Figure 5. The relationship between K_{ACh} channel open probability and the concentrations of GTP and ACh obtained by the improved integral model. (*a*) (i) The simulated time courses of activation and deactivation phases of 0.1, 0.3 and 3.0 μM ACh-induced K_G channel currents and $G_{\beta\gamma}$ on steps of various membrane voltages. (ii) Simulated time constants for activation and deactivation phases. (*b*) The relationship between the whole cell K_{ACh} current and ACh concentration. Symbols represent data from Kurachi *et al.* (1987), lines represent data obtained from the model at the indicated voltages. See text for further details.

course were evident. The deactivation of K_{ACh} current was faster at depolarized potentials than at hyperpolarized potentials. This phenomenon agrees with experimental results (half deactivation times of 6.3 ms at 0 mV and 15.7 ms at −80 mV; Ishii *et al.* 2001).

In figure 5*b*, the $[ACh]_0$ dependence of the steady state K_{ACh} current was calculated with the improved integrated model at various membrane potentials. The experimental data at −53 mV were taken from Kurachi *et al.* (1987; figure 5*b*, circles). Experimentally, as $[ACh]_0$ was increased, the whole cell K_{ACh} current was augmented in a concentration-dependent manner. The concentration–response relationship in the model was similar to the experimental data except at intermediate ACh concentrations (figure 5*b*, line −53 mV). Because the quasi-steady-state current was measured approximately 1 min after the onset of ACh application, the experimental data contain the effect of short-term desensitization. This may explain at least in part the difference between experimental data and the simulation data with the new model. The model results also suggest a novel possibility that the membrane potential affects the steady-state relationship between K_{ACh} current and $[ACh]_0$: as the membrane is more depolarized, the sensitivity of the K_{ACh} channel to ACh decreases. This possibility should be examined experimentally.

Downloaded from rsta.royalsocietypublishing.org on October 30, 2010

4. Discussion

This study presents the further development of a mathematical model to simulate the kinetics of G_K-protein signalling and the K_{ACh} current in the heart. This integrated model reproduced major characteristics of the K_{ACh} current, including steady-state relationships and temporal behaviour. Two experimental results played essential roles in the improvement of this model: (i) the biochemical assay of $G_{\beta\gamma}$ binding to K_{ACh} channels and (ii) the discovery of the involvement of RGSs in the control of the K_{ACh} channel activity.

Using these two key experimental advances, we improved the integrated model for ACh activation of the K_{ACh} channel (Hosoya *et al.* 1996; Hosoya & Kurachi 1999). Now with the new integrated model, we can reproduce the fast onset and offset of the K_{ACh} current upon application and removal of ACh. The calculated time constants for activation and deactivation are close to the physiological experimental data. However, we recognize that the activation of K_{ACh} current in experiments is yet faster than that of the model. We currently hypothesize that this may be related to the high affinity and low affinity properties of muscarinic receptors.

The deactivation time course of the simulated K_{ACh} current is quite in the physiological range. In simulation, as the membrane is depolarized, the deactivation becomes faster. This is also consistent with experimental observations reported in Ishii *et al.* (2001), and may be due to the higher GTPase accelerating activity of RGS proteins at depolarized potentials.

The simulated steady-state relationship between the K_{ACh} current and $[ACh]_0$ is shown in figure 5*b*. As the membrane is depolarized, the relationship shifts to the right and the maximal K_{ACh} channel activity is attenuated. This is also due to the higher activity of RGS proteins at depolarized potentials. But such an effect of the membrane potential on the relationship has not been yet reported *in vitro* and should be examined experimentally.

Models of processes associated with G-protein intracellular signalling may have practical applications. For example, an estimated 50 per cent of current pharmaceuticals target GPCR (Howard *et al.* 2001) and models may be useful tools to examine drug effects on G-protein signalling. The contributions of G-protein signalling to atrial fibrillation (AF) may be a good example. Hirose *et al.* showed that while $G_{\alpha q}$-TG mice activate the IP3 and DAG pathways and other intracellular signalling pathways to promote cellular hypertrophy, the over-expression of DAG kinase isoform DGKζ in the hearts of these mice prevented the generation of atrial arrhythmias including AF (Hirose *et al.* 2009). This suggests that therapies targeting Gαq and/or DAG-mediated signalling may prevent atrial arrhythmogenic remodelling and models of the appropriate signalling pathways in the atria may help to examine theoretical possibilities. The K_{ACh} current has been proposed to contribute to AF. Dobrev *et al.* (2005) and Cha *et al.* (2006) suggest that a constitutively active K_{ACh} current contributes to enhanced basal K^+ conductance and action potential shortening in chronic AF and blockade of the K_{ACh} current has become a new therapeutic target in AF. K_{ACh} channel blockers are under development and among them tertiapin and NIP-151 show effectiveness in terminating AF (Hashimoto *et al.* 2006, 2008). Differential phosphorylation-dependent regulation of the ion channel might underlie this constitutively active K_{ACh} current (Voigt *et al.* 2007). It will be interesting to use our model to

Downloaded from rsta.royalsocietypublishing.org on October 30, 2010

investigate possible sources of constitutive K_{ACh} channel activity—activation of K_{ACh} channels by GTP in the absence of ACh (Ito *et al.* 1991) and the loss of Ca^{2+}–CaM regulation of RGS proteins might prove to be attractive targets for further investigation. In which context it is interesting to note that knock-out of the RGS4 protein abolished desensitization of the response to ACh in the SA node in mice (Cifelli *et al.* 2008). A major limitation of the model presented here is that it cannot reproduce desensitization, and this after considerable effort. This may be because the model consists of linear systems subjected to a simple input (ACh concentration) which cannot reproduce a complex response such as desensitization. Further investigation of the function of RGS proteins may contribute to the understanding of sinus bradycardia.

Another limitation is that the experimental data used to develop the model were from different species (rat, guinea pig). Though the different expression levels of ion channels between species lead to different action potential forms, the characteristics of K_{ACh} channels in mammalian atrial myocytes do not seem to be so different and the species difference needs to be noted but it should not cause significant problems in the present modelling study which focuses on ion channel level phenomena.

In conclusion, progress in experimental research, such as the assay of $G_{\beta\gamma}$ binding to the K_{ACh} channels and the discovery of RGS proteins' action upon the K_{ACh} current, was essential for the development of this mathematical model for ACh activation of the K_{ACh} current. The simulation analyses raise further questions concerning the physiological behaviour of the K_{ACh} current, which indicates the necessity of new experiments. Experiments and simulation thus complement each other for the further understanding of physiological systems.

We thank Dr Ian Findlay (Université François-Rabelais, Tours, France) for critically reading this manuscript. This work was supported by the following research grants: Leading Project for Biosimulation 'Development of Models for Disease and Drug Action' to Y.K., Grant-in-Aid for Scientific Research on Priority Areas 17079005 to Y.K., Grant-in-Aid for Young Scientists (B) 20790206 to S.M. and the Global COE Program '*in silico* medicine' at Osaka University.

Appendix A

(*a*) *Allosteric model*

The $G_{K\beta\gamma}$ generated by the G_K protein cycle model was taken into the allosteric model and then the channel availability was calculated with the following equation:

$$NP_o = \frac{(1 + L(K_R/K_T)^4)(1 + ([G_{\beta\gamma}]/K_R))^4}{L(1 + (K_R/K_T)([G_{\beta\gamma}]/K_R))^4 + (1 + ([G_{\beta\gamma}]/K_R))^4}. \tag{A 1}$$

(*b*) *G-protein cycle model*

In the G_K-protein cycle model (figure 1*d*(ii)), six values of concentrations in the G-protein cycle are calculated with the following six ordinary differential

Downloaded from rsta.royalsocietypublishing.org on October 30, 2010

equations:

$$\frac{\mathrm{d[R]}}{\mathrm{d}t} = -k_1[\mathrm{A}][\mathrm{R}] + k_{-1}[\mathrm{AR}], \tag{A 2}$$

$$\begin{aligned}\frac{\mathrm{d[AR]}}{\mathrm{d}t} &= k_1[\mathrm{A}][\mathrm{R}] + k_{-2}[\mathrm{ARG{-}GDP}] + k_5[\mathrm{ARG{-}GTP}] \\ &\quad - k_{-1}[\mathrm{AR}] - k_2[\mathrm{AR}][\mathrm{G{-}GDP}],\end{aligned} \tag{A 3}$$

$$\begin{aligned}\frac{\mathrm{d[ARG{-}GDP]}}{\mathrm{d}t} &= -k_{-2}[\mathrm{ARG{-}GDP}] + k_2[\mathrm{AR}][\mathrm{G{-}GDP}] \\ &\quad - k_{3,4}[\mathrm{ARG{-}GDP}][\mathrm{GTP}] \\ &\quad + k_{-4,-3}[\mathrm{ARG{-}GTP}][\mathrm{GDP}],\end{aligned} \tag{A 4}$$

$$\begin{aligned}\frac{\mathrm{d[ARG{-}GTP]}}{\mathrm{d}t} &= k_{3,4}[\mathrm{ARG{-}GDP}][\mathrm{GTP}] \\ &\quad - k_{-4,-3}[\mathrm{ARG{-}GTP}][\mathrm{GDP}] \\ &\quad - k_5[\mathrm{ARG{-}GTP}],\end{aligned} \tag{A 5}$$

$$\frac{\mathrm{d[G{-}GTP]}}{\mathrm{d}t} = k_5[\mathrm{ARG{-}GTP}] - k_6[\mathrm{G{-}GTP}] \tag{A 6}$$

and

$$\begin{aligned}\frac{\mathrm{d[G{-}GDP]}}{\mathrm{d}t} &= k_6[\mathrm{G{-}GTP}] + k_{-2}[\mathrm{ARG{-}GDP}] \\ &\quad - k_2[\mathrm{AR}][\mathrm{G{-}GDP}],\end{aligned} \tag{A 7}$$

where A is ACh, R is m_2-receptor, G is G_K protein, and k are reaction rate constants. The value of each rate constant was fixed, except for k_6 (table 1). Since GTPase activity of $G_{K\alpha}$ in atrial myocytes can be modulated by RGS proteins in a voltage-dependent manner (Ishii *et al.* 2001), k_6 is defined as a function of membrane voltage as follows:

$$k_6 = 1.13\left(1 + \frac{1.30}{1 + \mathrm{e}^{(-0.042(V+25))}}\right), \tag{A 8}$$

where V is the membrane potential.

References

Akhter, S. A., Luttrell, L. M., Rockman, H. A., Iaccarino, G., Lefkowitz, R. J. & Koch, W. J. 1998 Targeting the receptor-Gq interface to inhibit *in vivo* pressure overload myocardial hypertrophy. *Science* **280**, 574–577. (doi:10.1126/science.280.5363.574)

Alemany, R., Perona, J. S., Sanchez-Dominguez, J. M., Montero, E., Canizares, J., Bressani, R., Escriba, P. V. & Ruiz-Gutierrez, V. 2007 G protein-coupled receptor systems and their lipid environment in health disorders during aging. *Biochim. Biophys. Acta* **1768**, 964–975. (doi:10.1016/j.bbamem.2006.09.024)

Barry, S. P., Davidson, S. M. & Townsend, P. A. 2008 Molecular regulation of cardiac hypertrophy. *Int. J. Biochem. Cell Biol.* **40**, 2023–2039. (doi:10.1016/j.biocel.2008.02.020)

Downloaded from rsta.royalsocietypublishing.org on October 30, 2010

Cha, T. J., Ehrlich, J. R., Chartier, D., Qi, X. Y., Xiao, L. & Nattel, S. 2006 Kir3-based inward rectifier potassium current: potential role in atrial tachycardia remodeling effects on atrial repolarization and arrhythmias. *Circulation* **113**, 1730–1737. (doi:10.1161/CIRCULATIONAHA.105.561738)

Cifelli, C., Rose, R. A., Zhang, H., Voigtlaender-Bolz, J., Bolz, S. S., Backx, P. H. & Heximer, S. P. 2008 RGS4 regulates parasympathetic signaling and heart rate control in the sinoatrial node. *Circ. Res.* **103**, 527–535. (doi:10.1161/CIRCRESAHA.108.180984)

Corey, S. & Clapham, D. E. 2001 The stoichiometry of Gβγ binding to G-protein-regulated inwardly rectifying K^+ channels (GIRKs). *J. Biol. Chem.* **276**, 11 409–11 413. (doi:10.1074/jbc.M100058200)

Demir, S. S., Clark, J. W. & Giles, W. R. 1999 Parasympathetic modulation of sinoatrial node pacemaker activity in rabbit heart: a unifying model. *Am. J. Physiol.* **276**, H2221–H2244.

Dobrev, D., Friedrich, A., Voigt, N., Jost, N., Wettwer, E., Christ, T., Knaut, M. & Ravens, U. 2005 The G protein-gated potassium current $I_{K,ACh}$ is constitutively active in patients with chronic atrial fibrillation. *Circulation* **112**, 3697–3706. (doi:10.1161/CIRCULATIONAHA.105.575332)

Faber, G. M. & Rudy, Y. 2007 Calsequestrin mutation and catecholaminergic polymorphic ventricular tachycardia: a simulation study of cellular mechanism. *Cardiovasc. Res.* **75**, 79–88. (doi:10.1016/j.cardiores.2007.04.010)

Felber, S., Breuer, H. P., Petruccione, F., Honerkamp, J. & Hofmann, K. P. 1996 Stochastic simulation of the transducin GTPase cycle. *Biophys. J.* **71**, 3051–3063. (doi:10.1016/S0006-3495(96)79499-7)

Feldman, D. S., Elton, T. S., Sun, B., Martin, M. M. & Ziolo, M. T. 2008 Mechanisms of disease: detrimental adrenergic signaling in acute decompensated heart failure. *Nat. Clin. Pract. Cardiovasc. Med.* **5**, 208–218. (doi:10.1038/ncpcardio1127)

Findlay, I., Suzuki, S., Murakami, S. & Kurachi, Y. 2008 Physiological modulation of voltage-dependent inactivation in the cardiac muscle L-type calcium channel: a modelling study. *Prog. Biophys. Mol. Biol.* **96**, 482–498. (doi:10.1016/j.pbiomolbio.2007.07.002)

Hao, N., Yildirim, N., Wang, Y., Elston, T. C. & Dohlman, H. G. 2003 Regulators of G protein signaling and transient activation of signaling: experimental and computational analysis reveals negative and positive feedback controls on G protein activity. *J. Biol. Chem.* **278**, 46 506–46 515. (doi:10.1074/jbc.M308432200)

Hashimoto, N., Yamashita, T. & Tsuruzoe, N. 2006 Tertiapin, a selective IK_{ACh} blocker, terminates atrial fibrillation with selective atrial effective refractory period prolongation. *Pharmacol. Res.* **54**, 136–141. (doi:10.1016/j.phrs.2006.03.021)

Hashimoto, N., Yamashita, T. & Tsuruzoe, N. 2008 Characterization of *in vivo* and *in vitro* electrophysiological and antiarrhythmic effects of a novel IK_{ACh} blocker, NIP-151: a comparison with an IKr-blocker dofetilide. *J. Cardiovasc. Pharmacol.* **51**, 162–169. (doi:10.1097/FJC.0b013e31815e854c)

Hendriks-Balk, M. C., Peters, S. L., Michel, M. C. & Alewijnse, A. E. 2008 Regulation of G protein-coupled receptor signalling: focus on the cardiovascular system and regulator of G protein signalling proteins. *Eur. J. Pharmacol.* **585**, 278–291. (doi:10.1016/j.ejphar.2008.02.088)

Hepler, J. R. 1999 Emerging roles for RGS proteins in cell signalling. *Trends Pharmacol. Sci.* **20**, 376–382. (doi:10.1016/S0165-6147(99)01369-3)

Hirose, M., Takeishi, Y., Niizeki, T., Shimojo, H., Nakada, T., Kubota, I., Nakayama, J., Mende, U. & Yamada, M. 2009 Diacylglycerol kinase ζ inhibits Gαq-induced atrial remodeling in transgenic mice. *Heart Rhythm* **6**, 78–84. (doi:10.1016/j.hrthm.2008.10.018)

Hosoya, Y. & Kurachi, Y. 1999 Functional analyses of G-protein activation of cardiac K_G channel. In *Potassium ion channels: molecular structure, function, and diseases* (eds Y. Kurachi, L. Y. Jan & M. Lazdunski). San Diego, CA: Academic Press.

Hosoya, Y., Yamada, M., Ito, H. & Kurachi, Y. 1996 A functional model for G protein activation of the muscarinic K+ channel in guinea pig atrial myocytes. Spectral analysis of the effect of GTP on single-channel kinetics. *J. Gen. Physiol.* **108**, 485–495. (doi:10.1085/jgp.108.6.485)

Downloaded from rsta.royalsocietypublishing.org on October 30, 2010

Howard, A. D., McAllister, G., Feighner, S. D., Liu, Q., Nargund, R. P., Van der Ploeg, L. H. & Patchett, A. A. 2001 Orphan G-protein-coupled receptors and natural ligand discovery. *Trends Pharmacol. Sci.* **22**, 132–140. (doi:10.1016/S0165-6147(00)01636-9)

Inanobe, A., Fujita, S., Makino, Y., Matsushita, K., Ishii, M., Chachin, M. & Kurachi, Y. 2001 Interaction between the RGS domain of RGS4 with G protein α subunits mediates the voltage-dependent relaxation of the G protein-gated potassium channel. *J. Physiol.* **535**, 133–143. (doi:10.1111/j.1469-7793.2001.t01-1-00133.x)

Ishii, M., Inanobe, A., Fujita, S., Makino, Y., Hosoya, Y. & Kurachi, Y. 2001 Ca^{2+} elevation evoked by membrane depolarization regulates G protein cycle via RGS proteins in the heart. *Circ. Res.* **89**, 1045–1050. (doi:10.1161/hh2301.100815)

Ishii, M., Inanobe, A. & Kurachi, Y. 2002 PIP3 inhibition of RGS protein and its reversal by Ca^{2+}/calmodulin mediate voltage-dependent control of the G protein cycle in a cardiac K^+ channel. *Proc. Natl Acad. Sci. USA* **99**, 4325–4330. (doi:10.1073/pnas.072073399)

Ito, H., Sugimoto, T., Kobayashi, I., Takahashi, K., Katada, T., Ui, M. & Kurachi, Y. 1991 On the mechanism of basal and agonist-induced activation of the G protein-gated muscarinic K+ channel in atrial myocytes of guinea pig heart. *J. Gen. Physiol.* **98**, 517–533. (doi:10.1085/jgp.98.3.517)

Katanaev, V. L. & Chornomorets, M. 2007 Kinetic diversity in G-protein-coupled receptor signalling. *Biochem. J.* **401**, 485–495. (doi:10.1042/BJ20060517)

Kurachi, Y. & Ishii, M. 2004 Cell signal control of the G protein-gated potassium channel and its subcellular localization. *J. Physiol.* **554**, 285–294. (doi:10.1113/jphysiol.2003.048439)

Kurachi, Y., Nakajima, T. & Sugimoto, T. 1986 Acetylcholine activation of K^+ channels in cell-free membrane of atrial cells. *Am. J. Physiol.* **251**, H681–H684.

Kurachi, Y., Nakajima, T. & Sugimoto, T. 1987 Short-term desensitization of muscarinic K^+ channel current in isolated atrial myocytes and possible role of GTP-binding proteins. *Pflugers Arch.* **410**, 227–233. (doi:10.1007/BF00580270)

Kurachi, Y., Ito, H., Sugimoto, T., Katada, T. & Ui, M. 1989 Activation of atrial muscarinic K^+ channels by low concentrations of $\beta\gamma$ subunits of rat brain G protein. *Pflugers Arch.* **413**, 325–327. (doi:10.1007/BF00583550)

Kurachi, Y., Ito, H. & Sugimoto, T. 1990 Positive cooperativity in activation of the cardiac muscarinic K^+ channel by intracellular GTP. *Pflugers Arch.* **416**, 216–218. (doi:10.1007/BF00370247)

Linderman, J. J. 2009 Modeling of G-protein-coupled receptor signaling pathways. *J. Biol. Chem.* **284**, 5427–5431. (doi:10.1074/jbc.R800028200)

Logothetis, D. E., Kurachi, Y., Galper, J., Neer, E. J. & Clapham, D. E. 1987 The $\beta\gamma$ subunits of GTP-binding proteins activate the muscarinic K+ channel in heart. *Nature* **325**, 321–326. (doi:10.1038/325321a0)

Logothetis, D. E., Kim, D. H., Northup, J. K., Neer, E. J. & Clapham, D. E. 1988 Specificity of action of guanine nucleotide-binding regulatory protein subunits on the cardiac muscarinic K+ channel. *Proc. Natl Acad. Sci. USA* **85**, 5814–5818. (doi:10.1073/pnas.85.16.5814)

Mackay, D. 1990 Interpretation of relative potencies, relative efficacies and apparent affinity constants of agonist drugs estimated from concentration-response curves. *J. Theor. Biol.* **142**, 415–427. (doi:10.1016/S0022-5193(05)80560-0)

Meij, J. T. 1996 Regulation of G protein function: implications for heart disease. *Mol. Cell. Biochem.* **157**, 31–38. (doi:10.1007/BF00227878)

Monod, J., Wyman, J. & Changeux, J. P. 1965 On the nature of allosteric transitions: a plausible model. *J. Mol. Biol.* **12**, 88–118. (doi:10.1016/S0022-2836(65)80285-6)

Mosser, V. A., Amana, I. J. & Schimerlik, M. I. 2002 Kinetic analysis of M2 muscarinic receptor activation of Gi in Sf9 insect cell membranes. *J. Biol. Chem.* **277**, 922–931. (doi:10.1074/jbc.M104210200)

Nakajima, T., Sugimoto, T. & Kurachi, Y. 1992 Effects of anions on the G protein-mediated activation of the muscarinic K+ channel in the cardiac atrial cell membrane. Intracellular chloride inhibition of the GTPase activity of GK. *J. Gen. Physiol.* **99**, 665–682. (doi:10.1085/jgp.99.5.665)

Downloaded from rsta.royalsocietypublishing.org on October 30, 2010

Ross, E. M. & Wilkie, T. M. 2000 GTPase-activating proteins for heterotrimeric G proteins: regulators of G protein signaling (RGS) and RGS-like proteins. *Annu. Rev. Biochem.* **69**, 795–827. (doi:10.1146/annurev.biochem.69.1.795)

Sakata, Y., Hoit, B. D., Liggett, S. B., Walsh, R. A. & Dorn II, G. W. 1998 Decompensation of pressure-overload hypertrophy in Gαq-overexpressing mice. *Circulation* **97**, 1488–1495.

Saucerman, J. J., Brunton, L. L., Michailova, A. P. & McCulloch, A. D. 2003 Modeling β-adrenergic control of cardiac myocyte contractility in silico. *J. Biol. Chem.* **278**, 47 997–48 003. (doi:10.1074/jbc.M308362200)

Semplicini, A. *et al.* 2006 Reduced expression of regulator of G-protein signaling 2 (RGS2) in hypertensive patients increases calcium mobilization and ERK1/2 phosphorylation induced by angiotensin II. *J. Hypertens.* **24**, 1115–1124. (doi:10.1097/01.hjh.0000226202.80689.8f)

Smith, N. J. & Luttrell, L. M. 2006 Signal switching, crosstalk, and arrestin scaffolds: novel G protein-coupled receptor signaling in cardiovascular disease. *Hypertension* **48**, 173–179. (doi:10.1161/01.HYP.0000232641.84521.92)

Suh, B. C., Horowitz, L. F., Hirdes, W., Mackie, K. & Hille, B. 2004 Regulation of KCNQ2/KCNQ3 current by G protein cycling: the kinetics of receptor-mediated signaling by Gq. *J. Gen. Physiol.* **123**, 663–683. (doi:10.1085/jgp.200409029)

Thomsen, W. J., Jacquez, J. A. & Neubig, R. R. 1988 Inhibition of adenylate cyclase is mediated by the high affinity conformation of the α 2-adrenergic receptor. *Mol. Pharmacol.* **34**, 814–822.

Voigt, N., Friedrich, A., Bock, M., Wettwer, E., Christ, T., Knaut, M., Strasser, R. H., Ravens, U. & Dobrev, D. 2007 Differential phosphorylation-dependent regulation of constitutively active and muscarinic receptor-activated $I_{K,ACh}$ channels in patients with chronic atrial fibrillation. *Cardiovasc. Res.* **74**, 426–437. (doi:10.1016/j.cardiores.2007.02.009)

Wieland, T. & Mittmann, C. 2003 Regulators of G-protein signalling: multifunctional proteins with impact on signalling in the cardiovascular system. *Pharmacol. Ther.* **97**, 95–115. (doi:10.1016/S0163-7258(02)00326-1)

Wieland, T., Lutz, S. & Chidiac, P. 2007 Regulators of G protein signalling: a spotlight on emerging functions in the cardiovascular system. *Curr. Opin. Pharmacol.* **7**, 201–207. (doi:10.1016/j.coph.2006.11.007)

Yi, T. M., Kitano, H. & Simon, M. I. 2003 A quantitative characterization of the yeast heterotrimeric G protein cycle. *Proc. Natl Acad. Sci. USA* **100**, 10 764–10 769. (doi:10.1073/pnas.1834247100)

Zhong, H., Wade, S. M., Woolf, P. J., Linderman, J. J., Traynor, J. R. & Neubig, R. R. 2003 A spatial focusing model for G protein signals. Regulator of G protein signaling (RGS) protein-mediated kinetic scaffolding. *J. Biol. Chem.* **278**, 7278–7284. (doi:10.1074/jbc.M208819200)

Am J Physiol Heart Circ Physiol 299: H680–H689, 2010.
First published July 2, 2010; doi:10.1152/ajpheart.00220.2009.

ANG II inhibits insulin-mediated production of PI 3,4,5-trisphosphates via a Ca^{2+}-dependent but PKC-independent pathway in the cardiomyocytes

Masashi Ikushima,[1,2] Masaru Ishii,[1] Mitsuru Ohishi,[2] Koichi Yamamoto,[2] Toshio Ogihara,[2] Hiromi Rakugi,[2] and Yoshihisa Kurachi[1]

Departments of [1]Pharmacology and [2]Geriatric Medicine, Osaka University Graduate School of Medicine, Osaka, Japan

Submitted 5 March 2009; accepted in final form 30 June 2010

Ikushima M, Ishii M, Ohishi M, Yamamoto K, Ogihara T, Rakugi H, Kurachi Y. ANG II inhibits insulin-mediated production of PI 3,4,5-trisphosphates via a Ca^{2+}-dependent but PKC-independent pathway in the cardiomyocytes. *Am J Physiol Heart Circ Physiol* 299: H680–H689, 2010. First published July 2, 2010; doi:10.1152/ajpheart.00220.2009.—Insulin resistance (IR) is a condition where different organs are refractory to insulin stimulation of glucose uptake. ANG II has been suggested to be involved in the development of IR in the heart. The precise mechanism by which this occurs is still unknown. Here we have used dynamic fluorescent imaging techniques to show that ANG II inhibits insulin production of phosphatidylinositol 3,4,5-trisphosphate [$PI(3,4,5)P_3$] in cardiac myocytes. Fluorophore (Venus)-conjugated cAMP-dependent protein kinase-pleckstrin homology domain, which specifically binds to $PI(3,4,5)P_3$, was transfected in neonatal rat cardiac myocytes. Insulin induced a robust increase in the fluorescence intensity at the cell surface, which was diminished by application of ANG II. The inhibitory action of ANG II was antagonized by RNH-6270 (an angiotensin type 1 receptor antagonist) but not by PD-122370 (an angiotensin type 2 receptor antagonist). BAPTA-AM (Ca^{2+} chelator) largely attenuated the ANG II effect, whereas K-252b (PKC inhibitor) did not. Furthermore, an elevation of intracellular Ca^{2+} induced by ionomycin mimicked the ANG II effect. Therefore, it is suggested that ANG II antagonizes insulin-mediated production of $PI(3,4,5)P_3$ via a Ca^{2+}-dependent but PKC-independent pathway in cardiac myocytes.

protein kinase C; angiotensin type 1 receptor; heart; adenosine 3′,5′-cyclic monophosphate-dependent protein kinase; real-time imaging; fluorophore

INSULIN IS ESSENTIAL FOR CONTROL of energy metabolism to maintain appropriate cellular homeostasis. A number of pathological factors severely attenuate the sensitivity to insulin in a variety of tissues, including skeletal muscle (43), adipocytes (6), and heart (1, 30, 39). This abnormal condition, called "insulin resistance" (IR), is known to be a predisposition or even a direct genesis of various common diseases, such as diabetes mellitus and atherosclerosis. In the heart, IR is reported to be critically involved in dysfunction of cardiac myocytes and closely related to some cardiac disorders (17, 30, 39).

The downstream signaling of insulin stimulation has been extensively studied (15, 23, 38). The stimulation of insulin receptor induces activation of phosphatidylinositol 3-kinase (PI 3-kinase) via insulin receptor substrate-1 (IRS-1). The active form of PI 3-kinase then generates phosphatidylinositol 3,4,5-trisphosphate [$PI(3,4,5)P_3$] from phosphatidylinositol 4,5-bisphosphate on the membrane (10). $PI(3,4,5)P_3$ can interact with the pleckstrin homology (PH) domain of a Ser/Thr kinase cAMP-dependent protein kinase (Akt)/PKB, which phosphorylates various downstream target molecules.

Recent studies have suggested that activation of ANG II type 1 receptor, AT_1, attenuates insulin signaling, and thus contributes to the pathogeneration of IR in various tissues (7, 36). Stimulation of AT_1 leads to activation of phospholipase C-β (PLC-β) (9) via a subtype of heterotrimeric G proteins, G_q (28, 35), and thus triggers phosphoinositide signaling cascades, which finally result in the elevation of intracellular Ca^{2+} concentration and activation of protein kinase C. A recent report showed that ANG II inhibits the insulin-mediated phosphorylation of Akt, a downstream signaling of $PI(3,4,5)P_3$, through PKC-α in vascular smooth muscle cells (VSMC) (22). The interaction between insulin and ANG II in cardiac myocytes, however, has not been well studied.

In this study, we examined the effects of insulin and ANG II on $PI(3,4,5)P_3$ in cardiac myocytes with dynamic visualization of $PI(3,4,5)P_3$. $PI(3,4,5)P_3$ is the product generated by insulin-mediated activation of PI 3-kinase and thus serves as a good indicator of insulin-mediated signaling cascades (5, 25, 27). For this purpose, we exploited a real-time imaging technique using a fluorophore-conjugated Akt-PH domain, which specifically binds to $PI(3,4,5)P_3$ in living cells. In result, we detected that ANG II competes insulin-mediated $PI(3,4,5)P_3$ production in a Ca^{2+}-dependent mechanism in cardiac myocytes. Application of BAPTA-AM (Ca^{2+} chelator), but not K-252b (PKC inhibitor), blocked the effect of ANG II. Ionomycin but not phorbol ester mimicked the effect of ANG II. Therefore, different from VSMC, ANG II may antagonize insulin action via a Ca^{2+}-dependent and PKC-independent pathway in cardiac myocytes.

MATERIALS AND METHODS

Reagents and plasmid. Insulin, ANG II, wortmannin, ionomycin, phorbol 12-myristate 13-acetate (PMA), and PD-123319 were all purchased from Sigma-Aldrich (St. Louis, MO). K-252b was purchased from BIOMOL International. 2-[*N*-(7-nitrobenz-2-oxa-1,3-diazol-4-yl)amino]-2-deoxy-D-glucose (2-NBDG) was purchased from Peptide Institute (Minoh, Osaka, Japan). RNH-6270, an active metabolite of olmesartan medoxomil, a specific AT_1 receptor antagonist, was supplied by Daiichi Sankyo (Tokyo, Japan). A fluorophore, Venus (kindly provided from Dr. Atsushi Miyawaki, RIKEN-BRC, Wako, Japan) fusioned construct with Akt-PH domain, was the generous gift from Dr. Tadaomi Takenawa (University of Tokyo, Tokyo, Japan). H9c2 cells, a clonal line derived from embryonic rat heart, were obtained from American Type Culture Collection (CRL-1446).

Cell dissociation and culture. All animal experiments were performed in accordance with the guidelines for the use of laboratory animals of the Osaka University Graduate School of Medicine. The

Address for reprint requests and other correspondence: H. Rakugi, Dept. of Geriatric Medicine, Osaka Univ. Graduate School of Medicine, 2-2 Yamadaoka, Suita, Osaka 565-0871, Japan (e-mail: rakugi@geriat.med.osaka-u.ac.jp).

0363-6135/10 Copyright © 2010 the American Physiological Society

Downloaded from ajpheart.physiology.org on October 30, 2010

study protocol was approved by our institution. Primary cultures of neonatal rat cardiac myocytes were prepared from the hearts of 1- to 2-day-old Wistar rats (Nippon Dobutsu, Osaka, Japan) as previously described (32). In brief, hearts were quickly removed from deeply anesthetized neonatal rats, minced, and digested with 0.125% trypsin (Becton-Dickinson, Sparks, MD) and 0.025% collagenase (Sigma-Aldrich) at 37°C for 1 h. Myocyte-enriched culture was achieved by preplating for 60 min to minimize the contamination of fibroblasts. Nonattached cells were then suspended in Hanks' medium-199 (M-199) (PAA Laboratories, Linz, Austria), supplemented with 10% FCS (Hyclone, Logan, UT), and cultured at 37°C in 99.5% air and 0.5% CO_2 for 1 day. The culture medium was changed to M-199 containing gentamycin and kanamycin (25 mg/l each) and then maintained for 2 days for the purpose of serum deprivation. On the next day, the medium was changed again and used for gene transfection. We performed immunostaining with α-actinin to confirm whether the isolated cells were cardiac myocytes. More than 95% of isolated cells were cardiac myocytes (data not shown).

Gene transfection. We applied Nucleofector (Amaxa Biosystems) for transient transfection of the Akt-PH-Venus gene. In brief, cardiac myocytes in medium 2×10^6 cells/ml were spun for 1 min at 340 *g*, and the cell pellet was resuspended in 100 μl Nucleofector solution. We mixed 100 μl of cell suspension with 2 μg of the Akt-PH-Venus plasmid, placed the sample in Nucleofector, and transfected the gene. Experiments evaluating insulin-mediated production of $PI(3,4,5)P_3$ under several conditions were performed within 24–48 h postnucleofection. Transfection efficiency of primary neonatal rat cardiac myocytes during this time period was ~50%, which was evaluated with cell numbers that were significantly positive with a fluorescence microscope.

Confocal microscopy imaging. Dynamic imaging was performed using laser scanning confocal microscopy (model LSM510; Carl Zeiss, Jena, Germany). The Axiovert 100 M microscope is equipped with a ×40 oil immersion objective (numeric aperture ~1.3). The Venus (a variant of yellow fluorescent protein) channel used the 488-nm line of an argon laser for excitation, and the emission wavelength was collected by a 500- to 535-nm bandpass filter for Venus.

Western blotting. Cell lysate was subjected to SDS-PAGE and was electrophoretically transferred to a nitrocellulose membrane (42). The membranes were then exposed to primary antibodies for Akt or phosphorylated (p)-Akt (dilution at 1:1,000; Cell Signaling Technology) overnight at 4°C. After incubation with the peroxidase-linked secondary antibody (dilution at 1:2,000; Cell Signaling Technology) for 1 h at room temperature, immunoreactive proteins were visualized by ECL PLUS reagent (Amersham Life Sciences).

Measurement of glucose uptake. To measure glucose uptake in rat cardiomyocytes (H9c2 cells), a nonradioactive assay was performed using a fluorescent D-glucose analog, 2-NBDG, as previously described (19, 41). Briefly, the cells plated on a 96-well plate at a density of 5,000 cells/well were serum depleted for 24 h. Next, the cells were incubated with the indicated drugs for 10 min, and 100 μM 2-NBDG

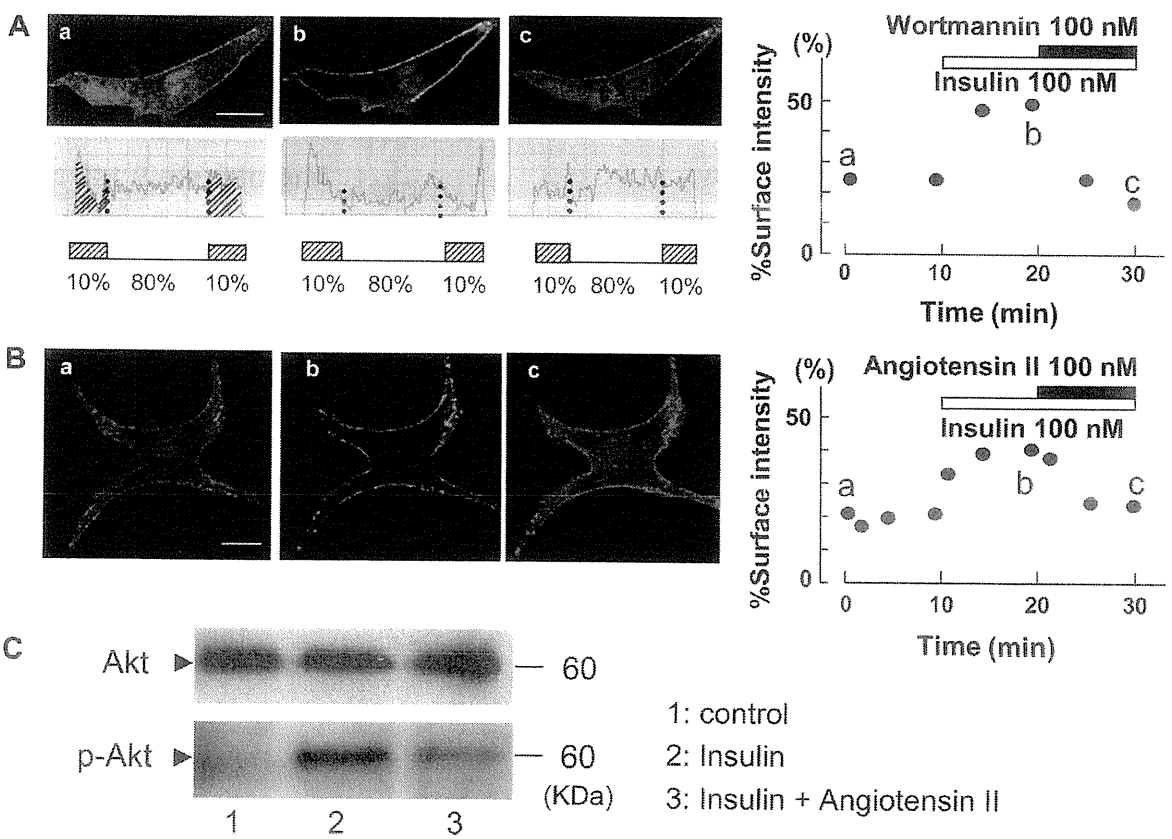

Fig. 1. Effects of ANG II on insulin signaling in cardiac myocytes. *A*: rat neonatal cardiac myocytes transfecting a fluorophore (Venus)-conjugated pleckstrin homology (PH) domain of cAMP-dependent protein kinase (Akt)/PKB were observed using a laser confocal microscope. Wortmannin prevents phosphatidylinositol trisphosphate production. *a*, In the basal state; *b*, cardiac myocyte after insulin (100 nM) application for 10 min; *c*, cardiac myocytes following wortmannin (100 nM) application for 10 min. *B*: fluorescence of Venus concentrated on application of insulin and ANG II. *a*, Cardiac myocyte in the basal state; *b*, cardiac myocyte after insulin (100 nM) application for 10 min; *c*, cardiac myocyte after ANG II (100 nM) application for 10 min. *C*: Western blotting of Akt or phosphorylated (p)-Akt in the cardiac myocyte on the application of insulin and ANG II. Panels on *right* indicate semiquantitative assessment of fluorescence. Surface intensity = intensity (10% from both edges)/total intensity. Scale bar indicates 10 μm.

Downloaded from ajpheart.physiology.org on October 30, 2010

was administrated to each well. After 10 min incubation, the cells were washed with PBS two times, and fluorescence was measured using a microplate reader (ARVOsx; PerkinElmer).

Statistical analysis. Statistical analysis was performed by Student's *t*-test. Statistical analysis for glucose uptake was performed by ANOVA, followed by Fisher's protected least-significant difference test using StatView (Abacus Concepts, Berkeley, CA). Results are expressed as means ± SE. A value of $P < 0.05$ was regarded significant.

RESULTS

Insulin-mediated PI(3,4,5)P_3 production on the cell membrane of cardiac myocytes. To visualize insulin signaling and to test the effects of ANG II on it in living cardiac myocytes, we used a real-time imaging technique that monitors the dynamics of PI(3,4,5)P_3, a membrane phospholipid generated by the insulin-signaling pathway. PH domain of Akt/PKB has been reported to strongly and specifically bind PI(3,4,5)P_3 (16, 31, 34). We therefore monitored the intensity/distribution of the fluorescence of a bright fluorophore, Venus, conjugated to the Akt-PH domain. Because of the improved speed and efficiency of maturation, the signal intensity of Venus is not affected by intracellular pH and not quenched by chloride ion. Therefore, the fluorophore is regarded as a powerful tool for tracking the movement of various substances in living cells (24).

We detected the fluorescence of the Venus-PH domain on the plasma membrane as well as in the cytosolic region in the control condition (Fig. 1*Aa*). This may indicate that a certain amount of PI(3,4,5)P_3 is constitutively present on the plasma membrane, even in the resting state. To evaluate the distribution of PI(3,4,5)P_3 in the cell, we vertically scanned the cell along a single line, as shown in Fig. 1*A*, and measured the intensity of fluorescence as the sum of pixels on the line (Fig. 1*A*, *bottom*). Next, we divided the sum of pixels within 10% from both edges with the total number of pixels on the line. We referred to this value as "percent surface intensity" (%SI). This value was used as a semiquantitative indicator reflecting the distribution of the fluorescence, i.e., PI(3,4,5)P_3, on the plasma membrane.

Application of insulin to the bath prominently enhanced the fluorescent signal at the cellular surface and its vicinity, although decreasing it in the cytosol (Fig. 1, *Aa* and *Ab*). This alteration gradually reached a plateau within 5 min, and %SI increased from 24 to 50 in this example (Fig. 1*A*, *right*). The increase of %SI was 95.2 ± 10.3% ($n = 10$, $P < 0.0001$). This translocation of the fluorescence of the Venus-PH domain from the cytosol to the plasma membrane region may be interpreted as indicating that insulin stimulates production of PI(3,4,5)P_3 in the close vicinity of plasma membrane in cardiac myocytes.

The plateau level of fluorescence was maintained constant during continuous presence of insulin at least for 40 min (data not shown). Treatment of the cardiac myocytes with wortmannin (100 nM), a blocker for PI 3-kinase, caused rapid redistribution of the fluorescence from the surface to the cytosol (Fig. 1*Ac*) (33, 37), and the %SI decreased to the level less than the control. The decrease of %SI was 46.1 ± 3.9% ($n = 5$, $P <$

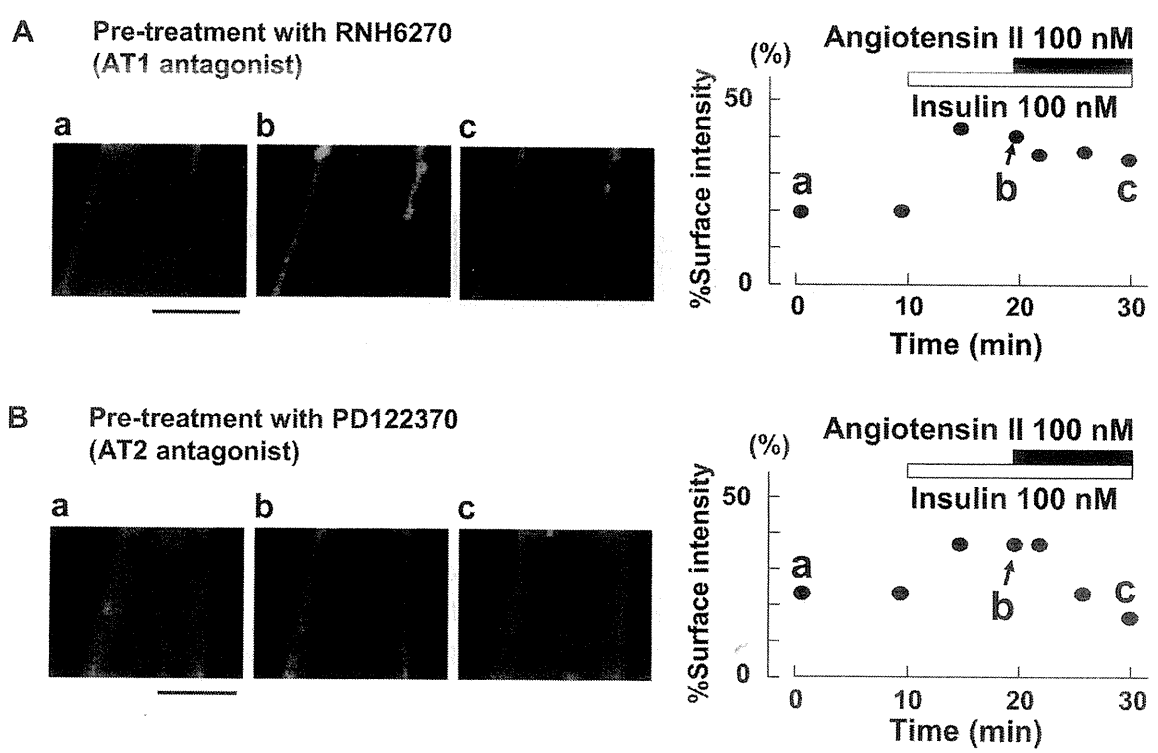

Fig. 2. ANG II antagonizes insulin signal via the angiotensin type 1 (AT_1) receptor. ANG II inhibits production of phosphatidylinositol 3,4,5-trisphosphate [PI(3,4,5)P_3] by insulin through AT_1 receptor but not the angiotensin type 2 (AT_2) receptor. Insulin (100 nM) was added at 30 min after RNH-6270 or PD-123319 application in the transfected myocyte medium, followed by ANG II (100 nM). *A* and *B*: effect of RNH-6270 (10 mM) and PD-123319 (10 mM). *a*, In the basal state; *b*, cardiac myocyte after insulin (100 nM) application for 10 min; *c*, cardiac myocyte following ANG II (100 nM) application for 10 min. Panels on *right* indicate quantitative assessment of fluorescence. Scale bar indicates 10 μm.

Downloaded from ajpheart.physiology.org on October 30, 2010

0.0001). This suggests that PI 3-kinase continued to produce $PI(3,4,5)P_3$ as long as insulin was present.

Inhibitory effect of ANG II on insulin-mediated production of $PI(3,4,5)P_3$ and phosphorylation of Akt through AT_1. We next examined the effect of ANG II on insulin-mediated translocation of the Venus-PH domain in cardiac myocytes (Fig. 1*B*). Insulin again caused the translocation of the Venus-PH domain from the cytosol to the plasma membrane region (Fig. 1*B*, *a* and *b*), and the %SI increased from 20 to 40 in this myocyte. ANG II (100 nM) further added to the bath reduced the fluorescence on the membrane region within 10 min almost to the initial level, and the %SI decreased to 25 in this example (Fig. 1*Bc*, *right*). The decrease of %SI after ANG II stimulation was 36.2 ± 3.9% ($n = 6$, $P < 0.0001$).

We next analyzed the phosphorylation of Akt/PKB (p-Akt) in cardiac myocytes induced by insulin by the Western blotting technique using an antibody specific to p-Akt. Because the phosphorylation of Akt requires the presence of $PI(3,4,5)P_3$, the p-Akt should be a good indicator for the active state of insulin signaling (3). Little signal of p-Akt was visible under control conditions (Fig. 1*C*, *bottom*, *lane 1*). The intensity of the band of p-Akt clearly increased in the presence of insulin (Fig. 1*C*, *bottom*, *lane 2*). When we treated the myocytes with the mixture of insulin (100 nM) and ANG II (100 nM), we detected a much less amount of p-Akt (Fig. 1*C*, *bottom*, *lane 3*). This result may indicate that ANG II inhibited the insulin-mediated production of $PI(3,4,5)P_3$ and thus decreased the amount of p-Akt. This is consistent with the fluorescent data using the Venus-Akt-PH domain in Fig. 1*B*. It is of note that neither insulin nor ANG II changed the amount of total Akt (Fig. 1*C*, *top*).

ANG II is known to exert its specific action by binding to either AT_1 receptor or angiotensin type 2 receptor (AT_2) that are coupled to G proteins (12, 20). When we preincubated the cells with a selective antagonist for AT_1 receptor, RNH-6270 (10 mM), ANG II could not interfere with the effect of insulin on $PI(3,4,5)P_3$ production on the plasma membrane (Fig. 2*A*, *a–c*). The %SI only marginally decreased from 40 to 35 in this example. Similar results were obtained in five different cardiac myocytes. The decrease of %SI was 4.5 ± 6.0% ($n = 6$, $P = 0.49$). On the other hand, ANG II could still block the insulin-mediated redistribution of the Venus-PH domain in the presence of PD-123319 (10 mM), a blocker specific for AT_2 (Fig. 2*B*, *a–c*). The %SI decreased from 40 to 18 in the example of Fig. 2*B*. The decrease of %SI was 32.9 ± 4.9% ($n = 5$, $P < 0.003$). These results strongly suggest that the inhibitory reaction of ANG II on insulin-mediated production of $PI(3,4,5)P_3$ occurs through AT_1 receptor, but not through AT_2.

Intracellular Ca^{2+} mobilization by ANG II is critically involved in inhibitory effects of ANG II on insulin-mediated $PI(3,4,5)P_3$ production. Compared with VSMC, little is known about the mechanism of IR mediated by ANG II signaling in cardiac myocytes. To clarify the mechanism of ANG II inhibition of insulin-mediated $PI(3,4,5)P_3$ production, we examined the role of inositol trisphosphate (IP_3) and diacylglycerol (DAG), which are known to be produced by ANG II via activation of PLC-β. We first examined the role of intracellular Ca^{2+}, which is released from endoplasmic reticulum by IP_3.

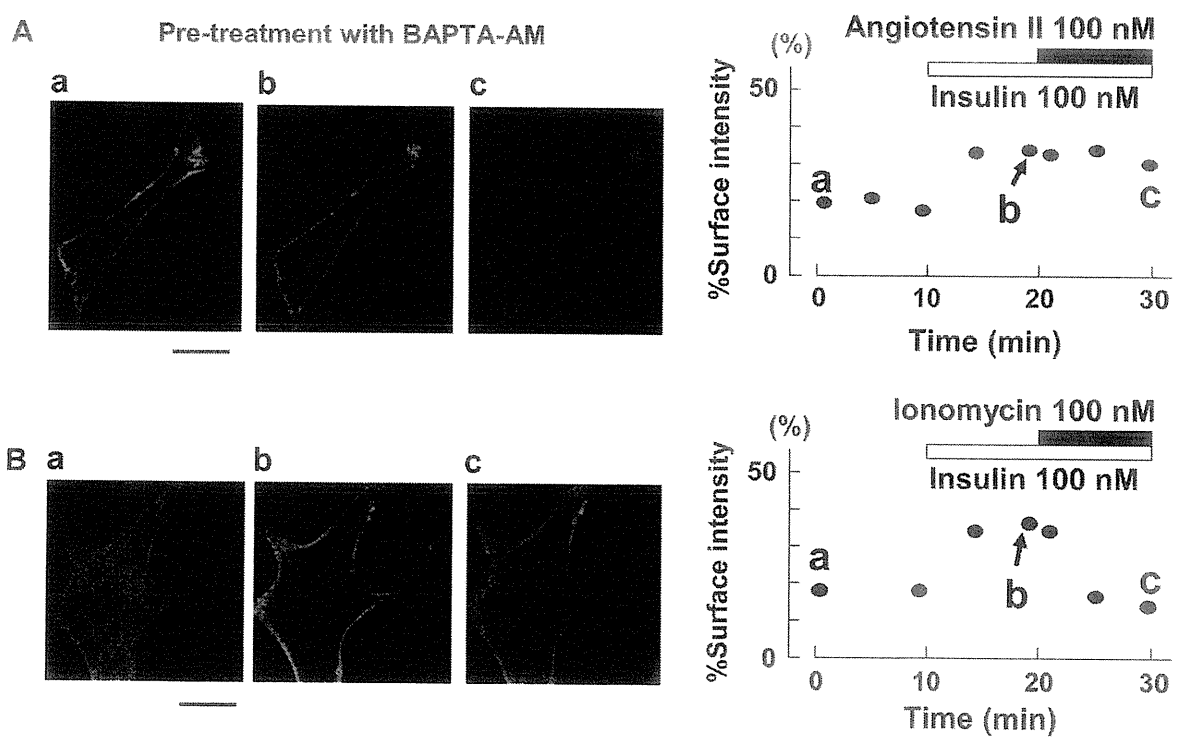

Fig. 3. ANG II antagonizes insulin signal through a Ca^{2+}-dependent pathway. *A*: intracellular Ca^{2+} chelator, BAPTA-AM (1 mM), was pretreated in the cardiac myocyte. *a*, In the basal state; *b*, cardiac myocyte after insulin (100 nM) application for 10 min; *c*, cardiac myocyte following ANG II (100 nM) application for 10 min. *B*: effect of ionomycin. *a*, In the basal state; *b*, cardiac myocyte after insulin (100 nM) application for 10 min; *c*, cardiac myocyte following ionomycin (100 nM) application for 10 min. Panels on *right* indicate quantitative assessment of fluorescence. Scale bar indicates 10 μm.

Downloaded from ajpheart.physiology.org on October 30, 2010

When we preincubated the cells with BAPTA-AM, a chelator of intracellular Ca^{2+}, ANG II could no longer inhibit the effect of insulin on the distribution of Venus-PH domain (Fig. 3*A*, *a–c*, *right*). The decrease of %SI after ANG II stimulation was 8.2 ± 7.6% (n = 4, P = 0.36). Conversely, application of the Ca^{2+} ionophore ionomycin (100 nM) instead of ANG II abolished insulin-mediated translocation of the fluorescence signal to the plasma membrane region (Fig. 3*B*, *a–c*, *right*). The decrease of

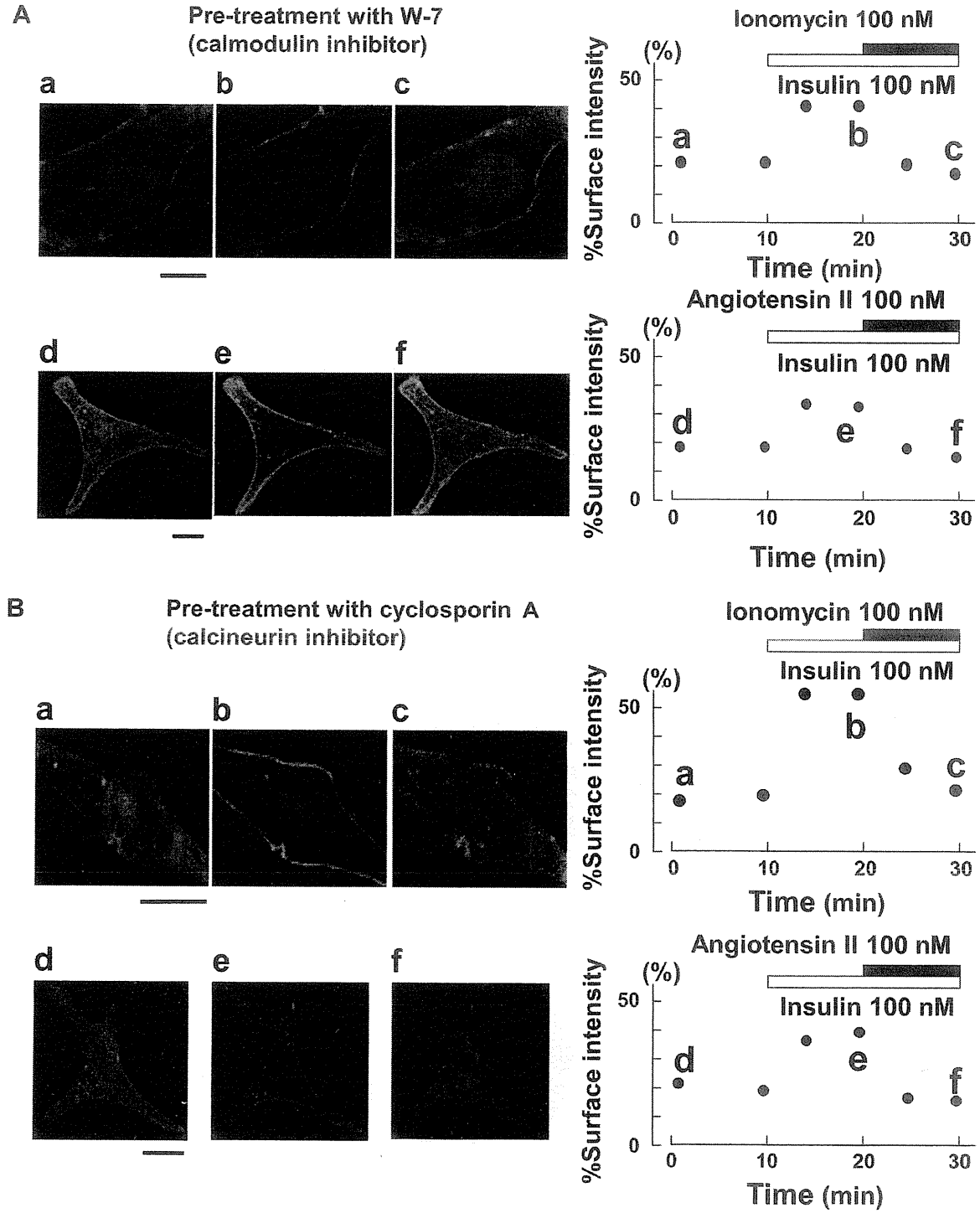

Fig. 4. Calmodulin and calcineurin have no effect of antagonizing insulin signaling. W-7 (calmodulin antagonist) or cyclosporine A (CyA, calcineurin antagonist) application was undertaken 30 min before insulin application. *A*: W-7 application (50 μM). *B*: CyA application (1 μM). *a* and *d*, In the basal state; *b*, cardiac myocyte after insulin application (100 nM) for 10 min; *c*, cardiac myocyte following ionomycin (100 nM) application; *e*, cardiac myocyte after ANG II application (100 nM) for 10 min; *f*, cardiac myocyte following ionomycin (100 nM) application. Panels on *right* indicate quantitative assessment of fluorescence. Scale bar indicates 10 μm.

Downloaded from ajpheart.physiology.org on October 30, 2010

%SI was 35.8 ± 3.6% (n = 5, P < 0.001). The time course of ionomycin action on insulin signaling resembled those of ANG II (see Fig. 1*B*). We also confirmed using the Ca^{2+} indicator fluo 3 that the application of ANG II caused the prominent Ca^{2+} mobilization in the cardiac myocytes (data not shown). Thus, it is suggested that an increase of intracellular Ca^{2+} by ANG II is critically involved in insulin-mediated PI(3,4,5)P_3 production. W-7, a specific blocker for calmodulin, and cyclosporine, a blocker of calcineurin, did not influence inhibition of the %SI of Venus-PH domain by ionomycin (Fig. 4, *A* and *B*), suggesting that these downstream signals may not be involved in the ANG II effect.

ANG II-induced activation of PKC is not essential for the inhibitory effect of ANG II on insulin-mediated PI(3,4,5)P_3 production. In vascular smooth muscles, it was shown that DAG-induced PKC activation by ANG II directly inhibits activation of IRS-1, which is considered to be a cause of ANG II-mediated IR (22). In addition, it is known that localized changes of intracellular Ca^{2+} determine the spatial and temporal targeting of PKC in smooth muscle cells (21). We therefore examined the effect of a PKC inhibitor, K-252b, on insulin-mediated PI(3,4,5)P_3 production in cardiac myocytes (Fig. 5). Pretreatment of the cells with K-252b (15 min) did not affect the inhibitory effect of either ionomycin or ANG II on the insulin-mediated increase of the %SI of Venus-PH domain (Fig. 5, *A* and *B*, respectively). The decrease of %SI was 29.6 ± 1.3% after stimulation with ionomycin (n = 3, P < 0.002) and 36.2 ± 3.3% after stimulation with ANG II (n = 4, P < 0.002). Accordingly, it is likely that intracellular Ca^{2+} elevation interferes with the action of insulin in a PKC-independent manner and that activation of PKC is not involved in ANG II-induced inhibition of insulin-mediated PI(3,4,5)P_3 production.

We next examined the effect of direct activation of endogenous PKC with the phorbol ester PMA. Insulin-mediated PI(3,4,5)P_3 production on the cell surface was only transiently inhibited by PMA (Fig. 6*A*). The transient decrease of %SI after PMA stimulation was 39.6 ± 5.7% (n = 5, P < 0.003). This effect was not observed after the application of an inactive form of PMA, 4α-PMA (data not shown). These results indicate that the activation of PKC has the rapid and transient interfering effect on the insulin-mediated PI(3,4,5)P_3 production. Chelating transient intracellular Ca^{2+} elevation by BAPTA-AM (Fig. 6*B*) did not block the effect of PMA, suggesting that this effect of PKC occurs independent of Ca^{2+} mobilization. The decrease of %SI after PMA stimulation was 34.6 ± 7.2% (n = 3, P < 0.04). These results suggest that the activation of PKC is insufficient to explain the sustained inhibitory effect of ANG II against the insulin-mediated PI(3,4,5)P_3 production in cardiac myocytes.

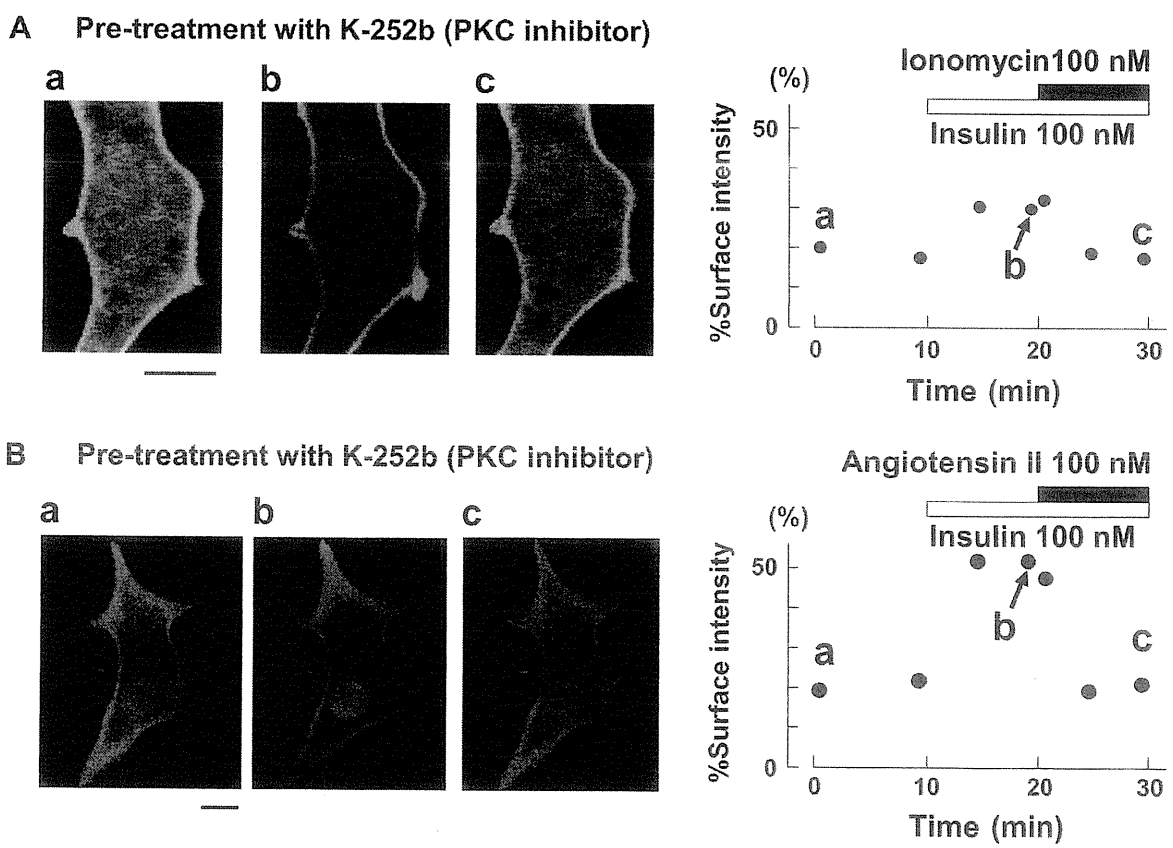

Fig. 5. Intracellular Ca^{2+} mobilization reduces PI(3,4,5)P_3 production mediated by insulin through a PKC-independent pathway. *A*: K-252b (100 μM) pretreatment 15 min before insulin application. *a*, In the basal state; *b*, cardiac myocyte after insulin (100 nM) application for 10 min; *c*, cardiac myocyte following ionomycin application (100 nM) for 10 min. *B*: K-252b (100 μM) pretreatment 15 min before insulin application. *a*, In the basal state; *b*, cardiac myocyte after insulin (100 nM) application for 10 min; *c*, cardiac myocyte following ANG II application (100 nM) for 10 min. Panels on *right* indicate quantitative assessment of fluorescence. Scale bar indicates 10 μm.

Downloaded from ajpheart.physiology.org on October 30, 2010

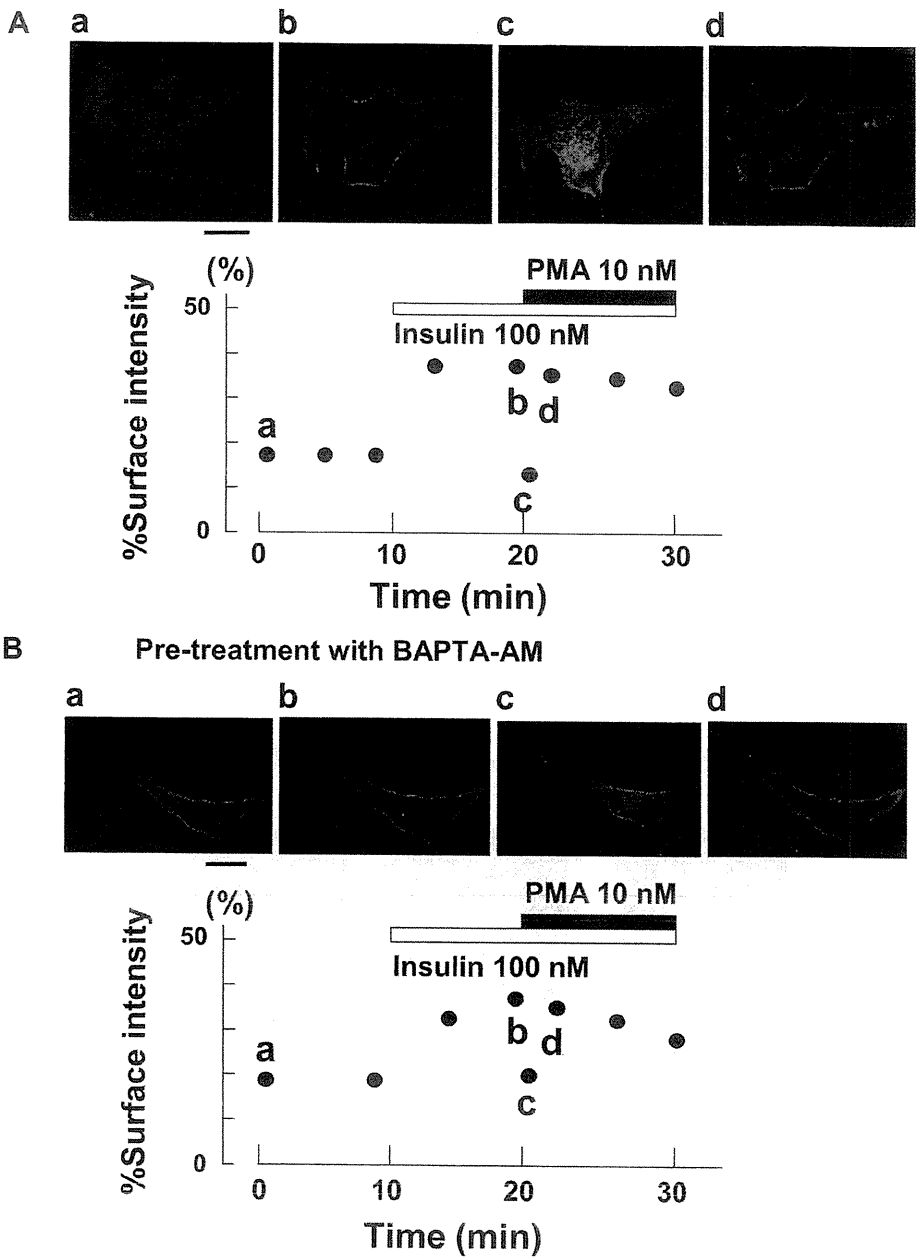

Fig. 6. Activation of PKC by phorbol 12-myristate 13-acetate (PMA) has rapid, transient antagonizing effects different from that observed with ANG II. *A*: no treatment. *B*: pretreatment with BAPTA-AM (1 mM). *a*, In the basal state; *b*, cardiac myocyte after insulin application (100 nM) for 10 min; *c*, cardiac myocyte then following PMA application (10 nM) for 10 s; *d*, cardiac myocyte then following PMA application (10 nM) for 1 min. Panels on *bottom* in *A* and *B* indicate quantitative assessment of fluorescence. Scale bar indicates 10 μm.

Inhibitory effect of ANG II on insulin-mediated glucose uptake was reversed through a Ca^{2+}-dependent pathway, but not through a PKC-dependent pathway. We confirmed whether the inhibitory effects of ANG II on insulin induced $PI(3,4,5)P_3$ production related to glucose uptake in cardiomyocytes. Insulin-mediated uptake of glucose in a clonal line of rat cardiomyocytes was measured using a fluorescent D-glucose derivative, 2-NBDG. ANG II inhibited insulin-mediated glucose uptake, which was reversed with BAPTA-AM, an intracellular Ca^{2+} chelator, but not with the PKC inhibitor K-2526 (Fig. 7). Changes in glucose uptake corresponded to changes in $PI(3,4,5)P_3$ production with these reagents.

DISCUSSION

ANG II inhibition of insulin signaling has been taken as one of the important mechanisms for the genesis of IR in various cells, including adipocytes (4, 26) and VSMC (22). Activation of PKC and an increase in intracellular Ca^{2+} are reported to be involved in ANG II-induced IR in adipocytes (2, 40) and VSMC (22). Although it was also reported that ANG II inhibits insulin signaling in cardiac myocytes (7, 36), its intracellular mechanisms remain unknown.

Using real-time imaging techniques with a fluorophore conjugated domain of Akt/PKB we analyzed the time course of changes in $PI(3,4,5)P_3$ concentration in the cardiac cell mem-

Downloaded from ajpheart.physiology.org on October 30, 2010

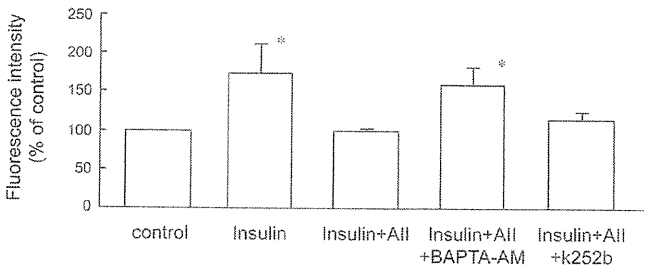

Fig. 7. Inhibitory effect of ANG II (AII) on insulin-mediated glucose uptake in rat cardiomyocyte was reversed through a Ca^{2+}-dependent pathway, but not through a PKC-independent pathway. Glucose uptake in H9c2 cells was measured using a fluorescent D-glucose derivative, 2-[*N*-(7-nitrobenz-2-oxa-1,3-diazol-4-yl)amino]-2-deoxy-D-glucose. Data are expressed as means ± SE of 3 experiments. BAPTA-AM, intracellular Ca^{2+} chelator; K-252b, PKC inhibitor, $*P < 0.05$ vs. control.

brane under various conditions. Both ANG II and ionomycin caused sustained inhibition of insulin-mediated $PI(3,4,5)P_3$ production. However, phorbol ester caused transient inhibition of insulin-mediated $PI(3,4,5)P_3$ production even though PKC activation was sustained under blocking the elevation of intracellular Ca^{2+} by BAPTA. These pharmacological investigations strongly suggest that ANG II-mediated inhibition of insulin signaling in cardiac myocytes is caused mainly by elevation of intracellular Ca^{2+} but not by activation of PKC. We have confirmed that this inhibitory effect of ANG II on insulin-mediated $PI(3,4,5)P_3$ production and the intracellular pathways corresponded with those on insulin-mediated glucose uptake.

On the contrary, in VSMC, the dominant signal to inhibit insulin-mediated Akt activation by ANG II is PKC-α but not intracellular Ca^{2+} (22). Therefore, the signal mechanism underlying ANG II inhibition of insulin signaling may vary according to cell types. Transient inhibition of insulin-mediated Akt activation by PMA in cardiomyocytes suggests activated PKC near the sarcolemma interfered with insulin signaling. However, this inhibitory effect of PMA was not sustained, and ANG II inhibition of insulin signaling was not suppressed by the PKC inhibitor in heart muscle cells. Taken together, we speculate that translocation of activated PKC to the sarcolemma is functional in VSMC but not in heart muscle cells.

Although we showed that the elevation of intracellular Ca^{2+} was involved in ANG II inhibition of insulin-mediated production of $PI(3,4,5)P_3$, we could not identify the signaling cascade following elevation of intracellular Ca^{2+}: W-7, a specific blocker for calmodulin, and cyclosporine, a blocker of calcineurin, did not influence inhibition of the %SI of Venus-PH domain by ionomycin (Fig. 4, *A* and *B*), suggesting that neither calmodulin nor calcineurin may be involved in the ANG II effect in cardiac myocytes.

There may be three possibilities for the downstream mechanism. First, we speculate the existence of unspecified molecules that cross talk with intracellular Ca^{2+} mobilization specifically in cardiac myocytes. The second possibility is that the target protein of PKC-α in VSMC is expressed at very low levels or absent in cardiac myocytes. The third possibility is that the levels of PKC activation by ANG II in our study might be insufficient to inhibit insulin signaling like as previously reported in PKC-transfected L6 muscle cells (8). Regarding the first possible mechanism, Jang et al. (13) speculated the existence of Ca^{2+}-dependent phosphatase because chelation of intracellular Ca^{2+} improved insulin sensitivity in high-fat-fed rats (13). Further studies are required to clarify the molecules that cross talk with intracellular Ca^{2+} mobilization in cardiac myocytes.

Insulin has close relationships with nutrition and energy metabolism. Between heart and vasculature, the importance of insulin signaling seems to be different because of different energy sources (11), i.e., free fatty acids for cardiac myocytes but glucose for VSMC. Although our studies were performed using nonfailing cardiomyocytes, the significance of insulin signaling in cardiac myocytes increases in the patients with heart failure because the development of heart failure induces crucial changes in energy source from fatty acid to glucose. It is reported that cardiac and plasma levels of ANG II increased in patients with heart failure (29). Taken together, clinical findings of usefulness of the renin-angiotensin blockers in patients with heart failure (18) may be explained in part through improvement of ANG II-mediated IR in cardiomyocytes of which energy source has changed to glucose. Exploration of the target molecules that cross talk with intracellular Ca^{2+} mobilization may lead to the further progress in the treatment of heart failure.

Study limitations. The first limitation of our study is that the analysis of the intensity of fluorophore is weak in quantification. We believe that %SI, which indicates the percent distribution of fluorophore in the edge site of whole fluorophore, is very useful to asses semiquantitatively the time course of changes in the distribution of fluorophore in response to pharmacological stimulation. Furthermore, the result of the quantitative analysis of glucose uptake was consistent with the semiquantitative result of the changes in $PI(3,4,5)P_3$ production.

The second limitation is that we could not make any conclusion about signaling pathways other than the ANG II-mediated pathway, such as the α-adrenergic receptor pathway that cross talks or overlaps with the insulin receptor signaling. Our previous experiment, however, indicates that the ANG II-mediated pathway plays a more important role than the α-adrenergic receptor pathway in hyperinsulinemia-induced cardiac hypertrophy of fructose-fed rats (14).

In summary, using the real-time imaging techniques, we have shown that ANG II may negatively regulate insulin-mediated $PI(3,4,5)P_3$ production via an increase of intracellular Ca^{2+} rather than via PKC activation through the stimulation of AT_1 receptor in the cardiac myocytes. The real-time imaging techniques may hold enormous potential to explore new cell signaling. The present finding indicates that the cardiomyocyte-specific interaction between insulin signaling and ANG II could be a new target for improving the metabolism of cardiomyocytes.

ACKNOWLEDGMENTS

We thank Dr. Tadaomi Takenawa (Univ. Tokyo, Tokyo, Japan) for providing the Akt-PH construct, Dr. Atsushi Miyawaki (RIKEN-BRC, Wako, Japan) for providing the Venus construct, and Dr. Katsuya Yamada (Hirosaki University Graduate School of Medicine, Hirosaki, Japan) for helpful suggestions in the experiment of glucose uptake.

GRANTS

This work was supported by the Leading Project for Biosimulation, "Development of models for disease and drug action" (to Y. Kurachi); by the Grant-in-Aid for Specific Research on Priority Area (12144207) (to Y. Kura-

Downloaded from ajpheart.physiology.org on October 30, 2010

chi); by the Grant-in-Aid for Scientific Research (A) (15209008) (to Y. Kurachi); by the Grant-in-Aid for the Encouragement of Young Scientists (15790133, 17790170) (to M. Ishii) from the Ministry of Education, Science, Sports and Culture of Japan; by a Uehara Memorial Research Grant (to Y. Kurachi); by the Japan Heart Foundation Dr. Hiroshi Irisawa Commemorative Research Grant (to M. Ishii); by the Grant-in-Aid from Ichiro Kanehara Foundation (to M. Ishii); by the Grant-in-Aid from Takeda Science Foundation (to M. Ishii); and by the Grant-in-Aid from Kanae Science Foundation (to M. Ishii).

DISCLOSURES

H. Rakugi reports receiving lecture fees from Daiichi Sankyo.

REFERENCES

1. **Alfarano C, Sartiani L, Nediani C, Mannucci E, Mugelli A, Cerbai E, Raimondi L.** Functional coupling of angiotensin II type 1 receptor with insulin resistance of energy substrate uptakes in immortalized cardiomyocytes (HL-1 cells). *Br J Pharmacol* 153: 907–914, 2008.
2. **Barthel A, Nakatani K, Dandekar AA, Roth RA.** Protein kinase C modulates the insulin-stimulated increase in Akt1 and Akt3 activity in 3T3–L1 adipocytes. *Biochem Biophys Res Commun* 243: 509–513, 1998.
3. **Burgering BM, Coffer PJ.** Protein kinase B (c-Akt) in phosphatidylinositol-3-OH kinase signal transduction. *Nature* 376: 599–602, 1995.
4. **Caldiz CI, de Cingolani GE.** Insulin resistance in adipocytes from spontaneously hypertensive rats: effect of long-term treatment with enalapril and losartan. *Metabolism* 48: 1041–1046, 1999.
5. **Currie RA, Walker KS, Gray A, Deak M, Casamayor A, Downes CP, Cohen P, Alessi DR, Lucocq J.** Role of phosphatidylinositol 3,4,5-trisphosphate in regulating the activity and localization of 3-phosphoinositide-dependent protein kinase-1. *Biochem J* 337: 575–583, 1999.
6. **Fasshauer M, Paschke R.** Regulation of adipocytokines and insulin resistance. *Diabetologia* 46: 1594–1603, 2003.
7. **Folli F, Saad MJ, Velloso L, Hansen H, Carandente O, Feener EP, Kahn CR.** Crosstalk between insulin and angiotensin II signalling systems. *Exp Clin Endocrinol Diabetes* 107: 133–139, 1999.
8. **Formisano P, Oriente F, Fiory F, Caruso M, Miele C, Maitan MA, Andreozzi F, Vigliotta G, Condorelli G, Beguinot F.** Insulin-activated protein kinase C-β bypasses Ras and stimulates mitogen-activated protein kinase activity and cell proliferation in muscle cells. *Mol Cell Biol* 20: 6323–6333, 2000.
9. **Griendling KK, Rittenhouse SE, Brock TA, Ekstein LS, Gimbrone MA Jr, Alexander RW.** Sustained diacylglycerol formation from inositol phospholipids in angiotensin II-stimulated vascular smooth muscle cells. *J Biol Chem* 261: 5901–5906, 1986.
10. **Harriague J, Bismuth G.** Imaging antigen-induced PI3K activation in T cells. *Nat Immunol* 3: 1090–1096, 2002.
11. **Hartil K, Charron MJ.** Genetic modification of the heart: transgenic modification of cardiac lipid and carbohydrate utilization. *J Mol Cell Cardiol* 39: 581–593, 2005.
12. **Horiuchi M, Hayashida W, Akishita M, Tamura K, Daviet L, Lehtonen JY, Dzau VJ.** Stimulation of different subtypes of angiotensin II receptors, AT1 and AT2 receptors, regulates STAT activation by negative crosstalk. *Circ Res* 84: 876–882, 1999.
13. **Jang YJ, Ryu HJ, Choi YO, Kim C, Leem CH, Park CS.** Improvement of insulin sensitivity by chelation of intracellular Ca(2+) in high-fat-fed rats. *Metabolism* 51: 912–918, 2002.
14. **Kamide K, Rakugi H, Higaki J, Okamura A, Nagai M, Moriguchi K, Ohishi M, Satoh N, Tuck ML, Ogihara T.** The renin-angiotensin and adrenergic nervous system in cardiac hypertrophy in fructose-fed rats. *Am J Hypertens* 15: 66–71, 2002.
15. **Kitamura T, Ogawa W, Sakaue H, Hino Y, Kuroda S, Takata M, Matsumoto M, Maeda T, Konishi H, Kikkawa U, Kasuga M.** Requirement for activation of the serine-threonine kinase Akt (protein kinase B) in insulin stimulation of protein synthesis but not of glucose transport. *Mol Cell Biol* 18: 3708–3717, 1998.
16. **Klippel A, Kavanaugh WM, Pot D, Williams LT.** A specific product of phosphatidylinositol 3-kinase directly activates the protein kinase Akt through its pleckstrin homology domain. *Mol Cell Biol* 17: 338–344, 1997.
17. **Lawlor MA, Alessi DR.** PKB/Akt: a key mediator of cell proliferation, survival and insulin responses? *J Cell Sci* 114: 2903–2910, 2001.
18. **Lee VC, Rhew DC, Dylan M, Badamgarav E, Braunstein GD, Weingarten SR.** Meta-analysis: angiotensin-receptor blockers in chronic heart failure and high-risk acute myocardial infarction. *Ann Intern Med* 141: 693–704, 2004.
19. **Leira F, Louzao MC, Vieites JM, Botana LM, Vieytes MR.** Fluorescent microplate cell assay to measure uptake and metabolism of glucose in normal human lung fibroblasts. *Toxicol In Vitro* 16: 267–273, 2002.
20. **Liu YH, Yang XP, Sharov VG, Nass O, Sabbah HN, Peterson E, Carretero OA.** Effects of angiotensin-converting enzyme inhibitors and angiotensin II type 1 receptor antagonists in rats with heart failure. Role of kinins and angiotensin II type 2 receptors. *J Clin Invest* 99: 1926–1935, 1997.
21. **Maasch C, Wagner S, Lindschau C, Alexander G, Buchner K, Gollasch M, Luft FC, Haller H.** Protein kinase C-α targeting is regulated by temporal and spatial changes in intracellular free calcium concentration $[Ca^{2+}]_i$. *FASEB J* 14: 1653–1663, 2000.
22. **Motley ED, Eguchi K, Gardner C, Hicks AL, Reynolds CM, Frank GD, Mifune M, Ohba M, Eguchi S.** Insulin-induced Akt activation is inhibited by angiotensin II in the vasculature through protein kinase C-α. *Hypertension* 41: 775–780, 2003.
23. **Myers MG Jr, Grammer TC, Wang LM, Sun XJ, Pierce JH, Blenis J, White MF.** Insulin receptor substrate-1 mediates phosphatidylinositol 3'-kinase and p70S6k signaling during insulin, insulin-like growth factor-1, and interleukin-4 stimulation. *J Biol Chem* 269: 28783–28789, 1994.
24. **Nagai T, Ibata K, Park ES, Kubota M, Mikoshiba K, Miyawaki A.** A variant of yellow fluorescent protein with fast and efficient maturation for cell-biological applications. *Nat Biotechnol* 20: 87–90, 2002.
25. **Oatey PB, Venkateswarlu K, Williams AG, Fletcher LM, Foulstone EJ, Cullen PJ, Tavare JM.** Confocal imaging of the subcellular distribution of phosphatidylinositol 3,4,5-trisphosphate in insulin- and PDGF-stimulated 3T3–L1 adipocytes. *Biochem J* 344: 511–518, 1999.
26. **Ogihara T, Asano T, Ando K, Chiba Y, Sakoda H, Anai M, Shojima N, Ono H, Onishi Y, Fujishiro M, Katagiri H, Fukushima Y, Kikuchi M, Noguchi N, Aburatani H, Komuro I, Fujita T.** Angiotensin II-induced insulin resistance is associated with enhanced insulin signaling. *Hypertension* 40: 872–879, 2002.
27. **Okada T, Kawano Y, Sakakibara T, Hazeki O, Ui M.** Essential role of phosphatidylinositol 3-kinase in insulin-induced glucose transport and antilipolysis in rat adipocytes. Studies with a selective inhibitor wortmannin. *J Biol Chem* 269: 3568–3573, 1994.
28. **Rockman HA, Koch WJ, Lefkowitz RJ.** Seven-transmembrane-spanning receptors and heart function. *Nature* 415: 206–212, 2002.
29. **Serneri GG, Boddi M, Cecioni I, Vanni S, Coppo M, Papa ML, Bandinelli B, Bertolozzi I, Polidori G, Toscano T, Maccherini M, Modesti PA.** Cardiac angiotensin II formation in the clinical course of heart failure and its relationship with left ventricular function. *Circ Res* 88: 961–968, 2001.
30. **Shah A, Shannon RP.** Insulin resistance in dilated cardiomyopathy. *Rev Cardiovasc Med* 4, *Suppl* 6: S50–S57, 2003.
31. **Shirai T, Tanaka K, Terada Y, Sawada T, Shirai R, Hashimoto Y, Nagata S, Iwamatsu A, Okawa K, Li S, Hattori S, Mano H, Fukui Y.** Specific detection of phosphatidylinositol 3,4,5-trisphosphate binding proteins by the PIP3 analogue beads: an application for rapid purification of the PIP3 binding proteins. *Biochim Biophys Acta* 1402: 292–302, 1998.
32. **Simpson P.** Stimulation of hypertrophy of cultured neonatal rat heart cells through an alpha 1-adrenergic receptor and induction of beating through an alpha 1- and beta 1-adrenergic receptor interaction. Evidence for independent regulation of growth and beating. *Circ Res* 56: 884–894, 1985.
33. **Smith LK, Vlahos CJ, Reddy KK, Falck JR, Garner CW.** Wortmannin and LY294002 inhibit the insulin-induced down-regulation of IRS-1 in 3T3–L1 adipocytes. *Mol Cell Endocrinol* 113: 73–81, 1995.
34. **Stokoe D, Stephens LR, Copeland T, Gaffney PR, Reese CB, Painter GF, Holmes AB, McCormick F, Hawkins PT.** Dual role of phosphatidylinositol-3,4,5-trisphosphate in the activation of protein kinase B. *Science* 277: 567–570, 1997.
35. **van Biesen T, Luttrell LM, Hawes BE, Lefkowitz RJ.** Mitogenic signaling via G protein-coupled receptors. *Endocr Rev* 17: 698–714, 1996.
36. **Velloso LA, Folli F, Sun XJ, White MF, Saad MJ, Kahn CR.** Cross-talk between the insulin and angiotensin signaling systems. *Proc Natl Acad Sci USA* 93: 12490–12495, 1996.
37. **Venkateswarlu K, Oatey PB, Tavare JM, Cullen PJ.** Insulin-dependent translocation of ARNO to the plasma membrane of adipocytes requires phosphatidylinositol 3-kinase. *Curr Biol* 8: 463–466, 1998.

Downloaded from ajpheart.physiology.org on October 30, 2010

38. **Wada T, Sasaoka T, Funaki M, Hori H, Murakami S, Ishiki M, Haruta T, Asano T, Ogawa W, Ishihara H, Kobayashi M.** Overexpression of SH2-containing inositol phosphatase 2 results in negative regulation of insulin-induced metabolic actions in 3T3–L1 adipocytes via its 5′-phosphatase catalytic activity. *Mol Cell Biol* 21: 1633–1646, 2001.
39. **Witteles RM, Tang WH, Jamali AH, Chu JW, Reaven GM, Fowler MB.** Insulin resistance in idiopathic dilated cardiomyopathy: a possible etiologic link. *J Am Coll Cardiol* 44: 78–81, 2004.
40. **Worrall DS, Olefsky JM.** The effects of intracellular calcium depletion on insulin signaling in 3T3–L1 adipocytes. *Mol Endocrinol* 16: 378–389, 2002.
41. **Yamada K, Nakata M, Horimoto N, Saito M, Matsuoka H, Inagaki N.** Measurement of glucose uptake and intracellular calcium concentration in single, living pancreatic beta-cells. *J Biol Chem* 275: 22278–22283, 2000.
42. **Yang J, Matsukawa N, Rakugi H, Imai M, Kida I, Nagai M, Ohta J, Fukuo K, Nabeshima Y, Ogihara T.** Upregulation of cAMP is a new functional signal pathway of Klotho in endothelial cells. *Biochem Biophys Res Commun* 301: 424–429, 2003.
43. **Zierath JR, Krook A, Wallberg-Henriksson H.** Insulin action and insulin resistance in human skeletal muscle. *Diabetologia* 43: 821–835, 2000.

Downloaded from ajpheart.physiology.org on October 30, 2010

IBMS BoneKEy. 2010 August;7(8):279-286
http://www.bonekey-ibms.org/cgi/content/full/ibmske;7/8/279
doi: 10.1138/20100459

PERSPECTIVES

Control of Osteoclast Precursor Migration: A Novel Point of Control for Osteoclastogenesis and Bone Homeostasis

Taeko Ishii, Junichi Kikuta, Atsuko Kubo and Masaru Ishii

Laboratory of Biological Imaging, WPI-Immunology Frontier Research Center, Osaka University, Suita, Japan

Abstract

Osteoclasts are bone-resorbing, multinucleated giant cells that differentiate from mononuclear macrophage/monocyte-lineage hematopoietic precursors. They have critical roles not only in normal bone remodeling but also during pathogenesis of destructive bone disorders such as osteoporosis, rheumatoid arthritis, and cancers metastatic to bone. Many molecules, especially macrophage colony-stimulating factor (M-CSF) and receptor activator of nuclear factor κB ligand (RANKL), make significant contributions to osteoclast differentiation. However, the process of osteoclast precursor trafficking to and from the bone surface, where cell fusion occurs to form the fully differentiated multinucleated cells that mediate bone resorption, is less well-documented. Recent studies have shed light on the mechanisms involved and have demonstrated the vital participation of various chemokines such as CCL2, CCL5, CXCL12, and CX_3CL1, and lipid mediators such as sphingosine-1-phosphate (S1P). In addition, advances in imaging technologies, such as the development of intravital multiphoton microscopy, have enabled the *in situ* visualization of the behavior of osteoclasts and their precursors within intact bone tissue. This capability will be extremely useful for dissecting the mechanisms controlling the migration of these cells *in vivo*. In this *Perspective*, we review the latest knowledge in this new field of bone biology, with a focus on novel imaging methodology and its applications in this field. *IBMS BoneKEy*. 2010 August;7(8):279-286.
©2010 International Bone & Mineral Society

Introduction

Bone is a dynamically regulated tissue that continuously undergoes remodeling to maintain mineral homeostasis and structural robustness. The balance between bone resorption by osteoclasts and bone formation by osteoblasts is finely regulated (1-3), and several complex mechanisms maintain this equilibrium. The mechanism that has been investigated most extensively is the control of both osteoclast and osteoblast differentiation (1;2;4). Recently, the regulation of precursor cell recruitment has attracted attention (5-14). We have also investigated extensively the highly organized migration of osteoclast precursors between the bone marrow and blood vessels, in real-time using intravital multiphoton microscopy (14;15). In this review, we summarize recent findings regarding the recruitment of osteoclast precursor cells to the bone surface and briefly introduce *in vivo* imaging of bone.

What Are Osteoclasts? Where Do They Come From, and Where Are They Going?

Even in adults who have completed their growth, osseous tissue is continuously remodeled via bone resorption by osteoclasts and bone formation by osteoblasts, to maintain bone strength and electrolyte balance. In several pathological states, including osteoporosis, tumor-induced osteolysis, and rheumatoid arthritis, osteoclasts are activated excessively, and the balance between bone formation and resorption is disrupted. Consequently, the inhibition of osteoclast function is a major therapeutic target in these diseases (3).

The osteoclast is a unique multinucleated giant cell formed by the fusion of mononuclear precursors of the macrophage-

Copyright 2010 International Bone & Mineral Society

monocyte lineage. The differentiation of precursor cells into mature osteoclasts requires two important molecules: macrophage colony-stimulating factor (M-CSF) and receptor activator of nuclear factor κB ligand (RANKL) (16-18). In addition, although this is still controversial, it has been reported that many hormones, cytokines, and growth factors such as parathyroid hormone, estrogen, 1,25-dihydroxyvitamin D_3, and interleukin-6 can affect osteoclast differentiation by regulating the expression of M-CSF, RANKL, and osteoprotegerin, a non-signaling decoy receptor for RANKL (1-3). The major source of M-CSF, RANKL, and osteoprotegerin in bone tissue is osteoblastic lineage cells, or stromal cells, and the interaction between osteoclast and osteoblast lineages is critical in bone homeostasis (1-3). Signaling also occurs in the opposite direction. Stimulatory factors such as transforming growth factor-β, insulin-like growth factor-1, and cardiotrophin-1 are released from osteoclasts during bone resorption and stimulate bone formation by osteoblasts (4). In addition, EphrinB2 expressed by osteoclasts and EphB4 expressed by osteoblasts participate in bidirectional communication between osteoclast- and osteoblast-lineage cells (19).

The mechanism by which osteoclast precursors are recruited at the proper time to appropriate sites for differentiation is unclear. The bone marrow cavity and bloodstream contain monocyte-lineage precursor cells, which can differentiate into osteoclast precursor cells. These precursors are recruited to the surface of bone, where they differentiate into mature osteoclasts. Moreover, cell cycle-arrested quiescent osteoclast precursors on the bone surface can differentiate into mature osteoclasts upon exposure to several stimuli (22). Although the differentiation stage at which osteoclast precursor cells migrate to the bone surface is controversial, several cytokines were shown recently to be involved in their recruitment (5-13). In addition to *in vitro* migration assays, intravital two-photon imaging permits the observation of cell behavior *in vivo* in real-time and is a powerful tool for determining spatiotemporal control mechanisms (15;23;24). Below, we review recent findings from many groups, including ours, regarding the recruitment and release of osteoclast precursors.

Attractants and Repellents

Although the mechanism of osteoclast precursor recruitment remains elusive, several chemoattractants and chemorepellants have been shown to play critical roles in controlling the migration of monocyte-lineage precursor cells from blood vessels into the bone marrow cavity. As with leukocytes, the migration of osteoclast precursors is regulated mainly by short peptides (approximately 70-90 amino acids) known as chemokines. Chemokines have been classified into C, CC, CXC, and CX3C subfamilies, according to their structural cysteine motif. Chemokine receptors are G protein-coupled receptors (GPCRs, also known as seven-transmembrane receptors), and act specifically through pertussis toxin (PTx)-sensitive Gαi components. Although some chemokine-receptor pairs are exclusive, most receptors interact with multiple ligands, and most ligands interact with more than one receptor. This redundancy makes their regulation complex (25). The best-known chemoattractant is CXCL12 (or stromal derived factor-1, SDF-1), a CXCR4 ligand (5;6). CXCL12 is expressed constitutively at high levels within bone by osteoblastic stromal cells and vascular endothelial cells, while CCR4 is expressed on a wide variety of cells, including circulating monocytes and osteoclast precursors. CXCL12 has chemotactic effects on osteoclast precursors, which express high levels of CCR4 (5). Recently, another chemokine, CX_3CL1 (or fractalkine), which works as an adhesion molecule as a membrane-bound chemokine, and as a chemoattractant after being cleaved by ADAM10 and ADAM17. CX_3CL1, which is the only known member of the CX3C subfamily and expressed by osteoblastic stromal cells, was reported to be involved in both the recruitment and attachment of osteoclast precursors (7). These cytokines are engaged mainly in the interaction between osteoclasts and

Copyright 2010 International Bone & Mineral Society